Supplementary material

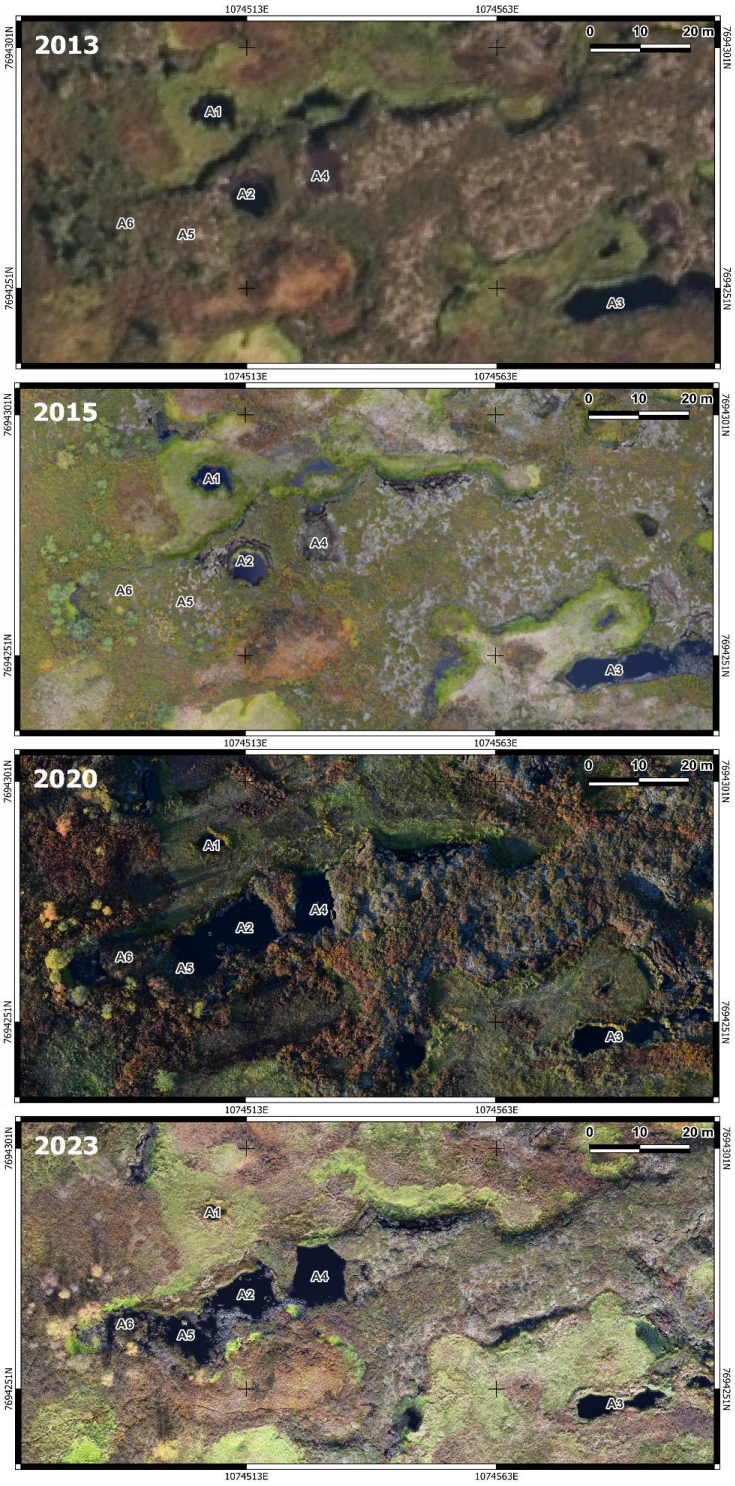

Figure S1: Aerial images of the main study area in Áidejávri (A1-A6) from 2013 to 2023 illustrate the degradation of the peat plateau. The aerial image from 2013 was obtained from the Norwegian Mapping Authority (Norgeibilder.no, 2025), while orthophotos from 2015, 2020, and 2023 were made through drone surveys and processed following the method described in Martin et al., 2021. The figure illustrates that the thermokarst pond formation age was identified as the time of permafrost collapse and not the start of water accumulation, as demonstrated in the case of pond A4. In pond A4, the

permafrost started to collapse in 2013, and the pond was already established by 2020. Thus, the approximate age of the pond has been identified as 7 years as of 2023. Coordinate system is EPSG25832: ETRS89/UTM zone 32N.

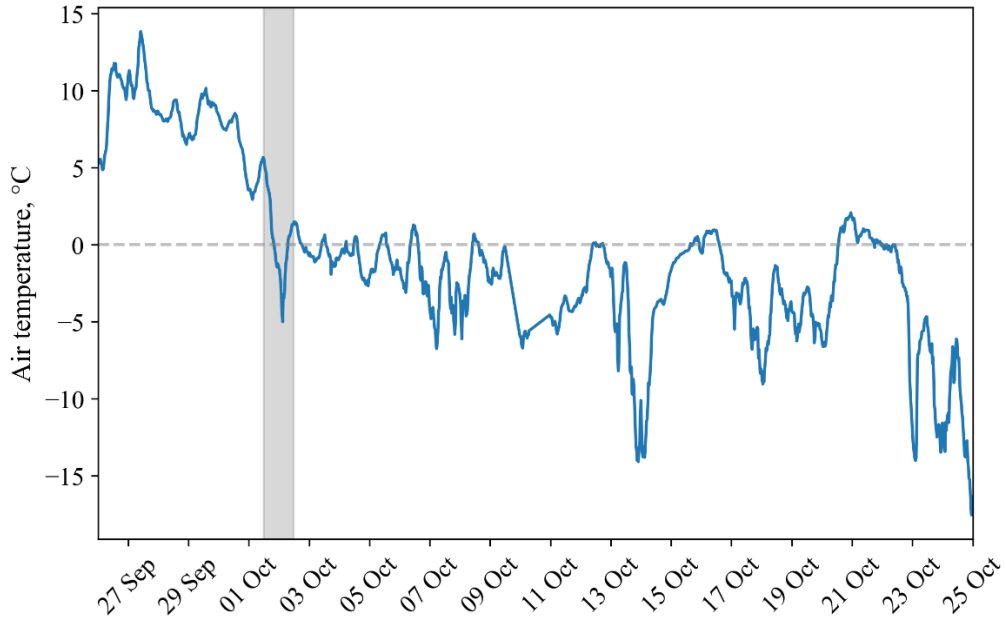

Figure S2. Air temperature measured from September 26, 2023, to October 25, 2023, using a resistance temperature detector (PT-100) located in a radiation shield at 2 m above ground level (a.g.l.) on the eddy covariance tower in Iškoras (Pirk et al., 2024). The beginning of ice formation in 2023 is shown with grey shading.

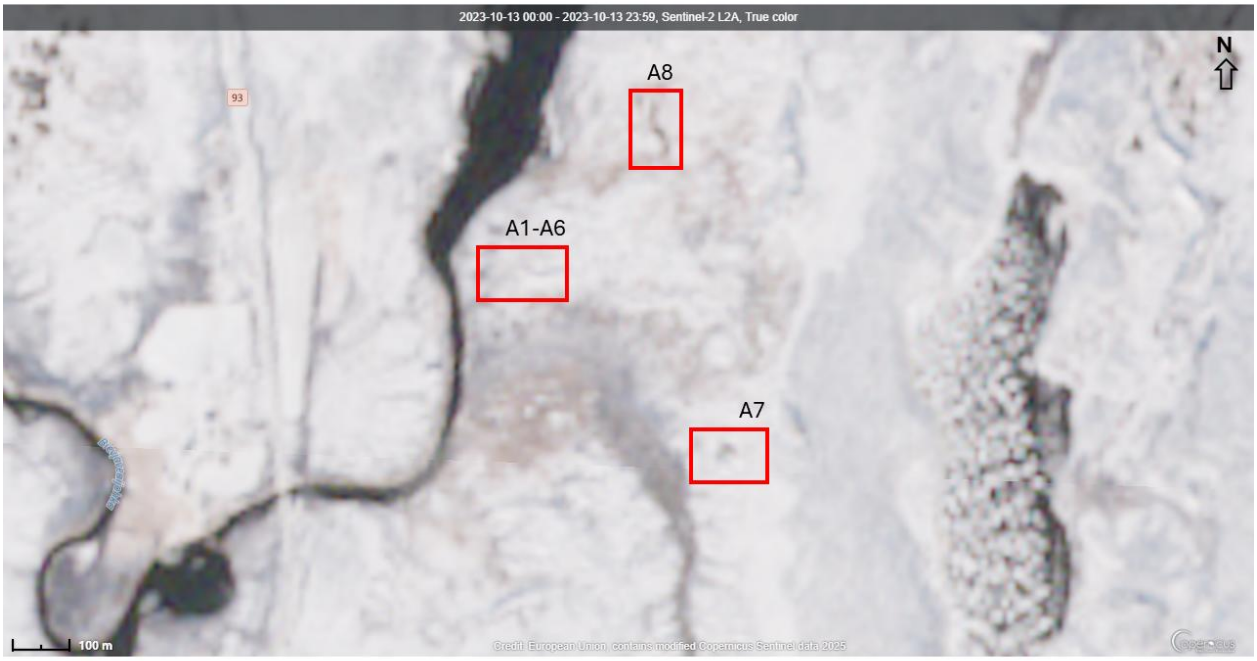

Figure S3. Sentinel-2 L2A image of the Áidejávri area taken on October 13, 2023, from Copernicus Data Browser, https://browser.dataspace.copernicus.eu/ (accessed September 2024 and May 2025). The studied ponds in Áidejávri are indicated with red rectangles. The image shows that, by October 13, the ponds in Áidejávri were ice-covered.

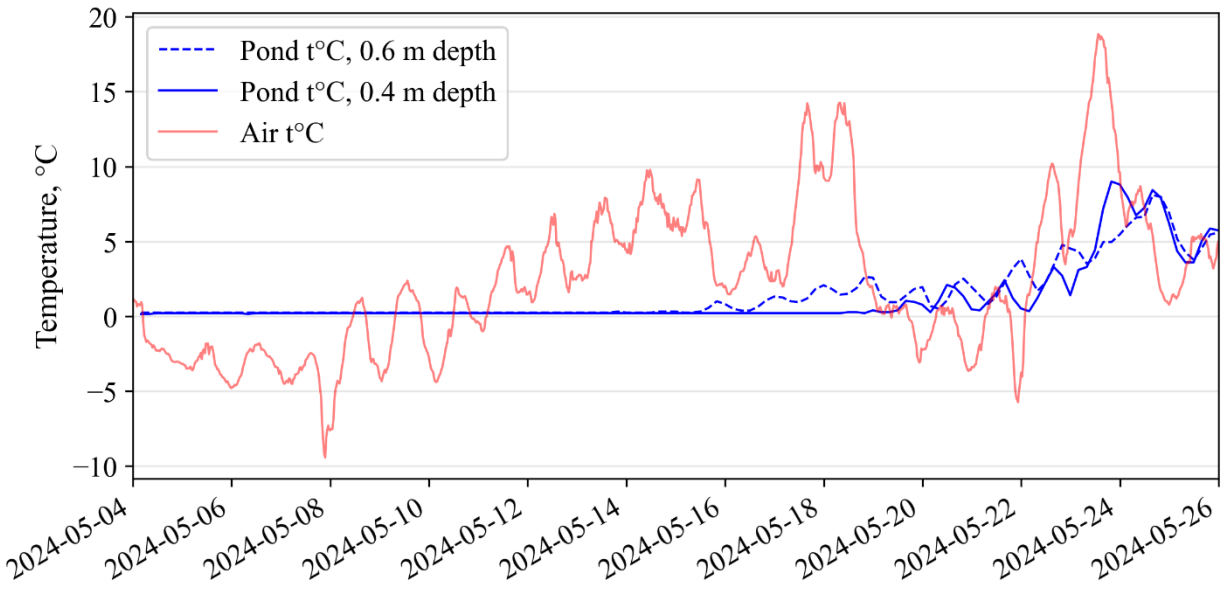

Figure S4. Air and water temperatures of the pond at Iškoras (Isk) measured between May 4 and May 26, 2024. Water temperatures were recorded using automatic data loggers (iButton) at two depths: 0.4 m and 0.6 m (bottom). Air temperature was measured with a resistance temperature detector (PT-100) located in a radiation shield at 2 m above ground level (a.g.l.) on the eddy covariance tower in Iškoras (Pirk et al., 2024).

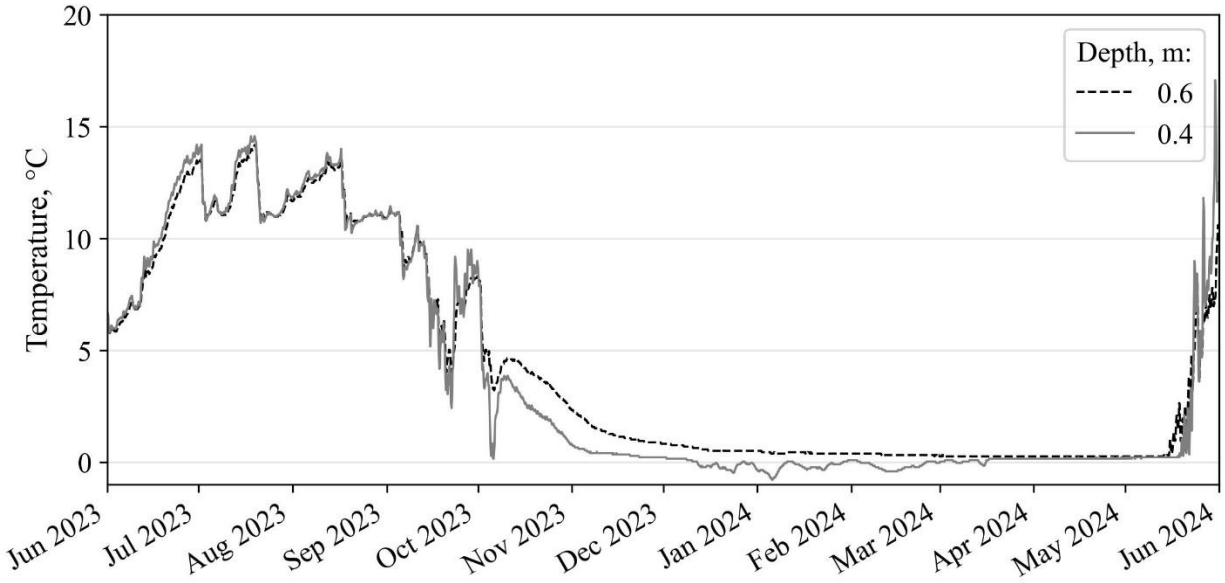

Figure S5. Water temperature measured in pond Isk at Iškoras at two depths: 0.4 m and 0.6 m (bottom). Temperatures were recorded using automatic data loggers (iButton).

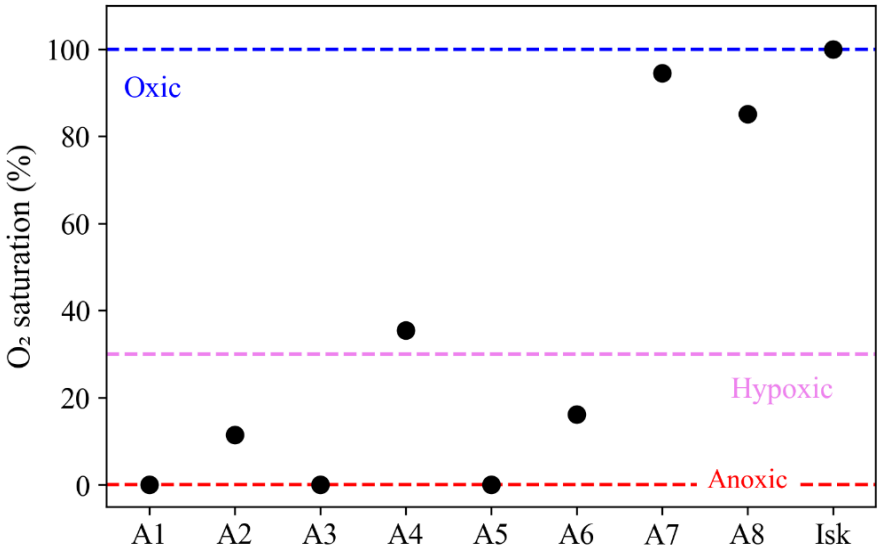

Figure S6. Oxygen saturation in surface water during September 2024 relative to atmospheric equilibrium. Oxygen conditions are classified as oxic (more than 30 %), hypoxic (below 30 %), and as anoxic when saturation values were below 1 %. We estimated a high absolute error of 20 % in oxygen saturation measurements due to significant differences observed between measured values in replicate samples.

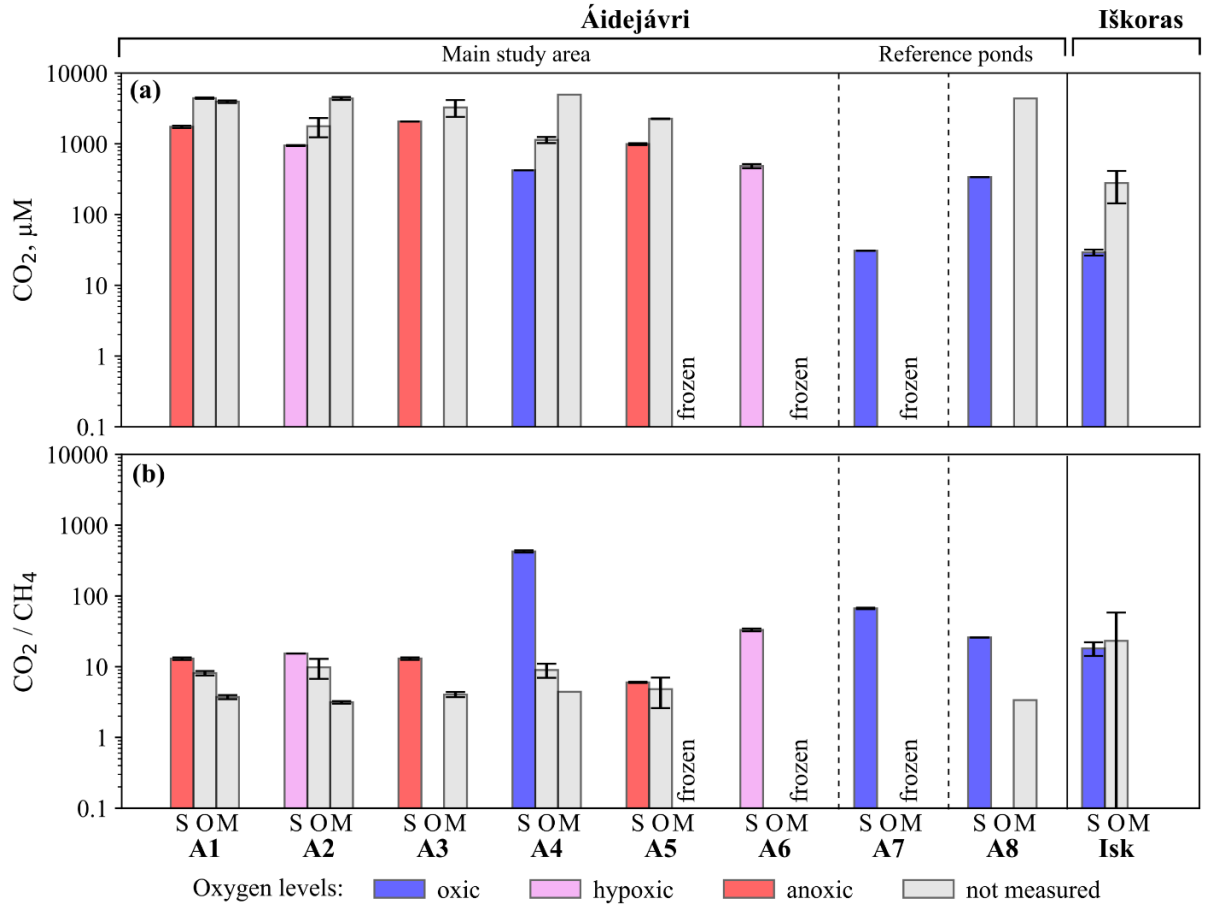

Figure S7. Dissolved CO_2 concentrations (a) and CO_2/CH_4 ratio (b) in the unfrozen water column of the studied ponds across each season (March - M, September - S, and October - O, 2024). Error bars represent the standard deviations of multiple samples collected from different depths in March and October, as well as replicate samples taken in September from the same depth.

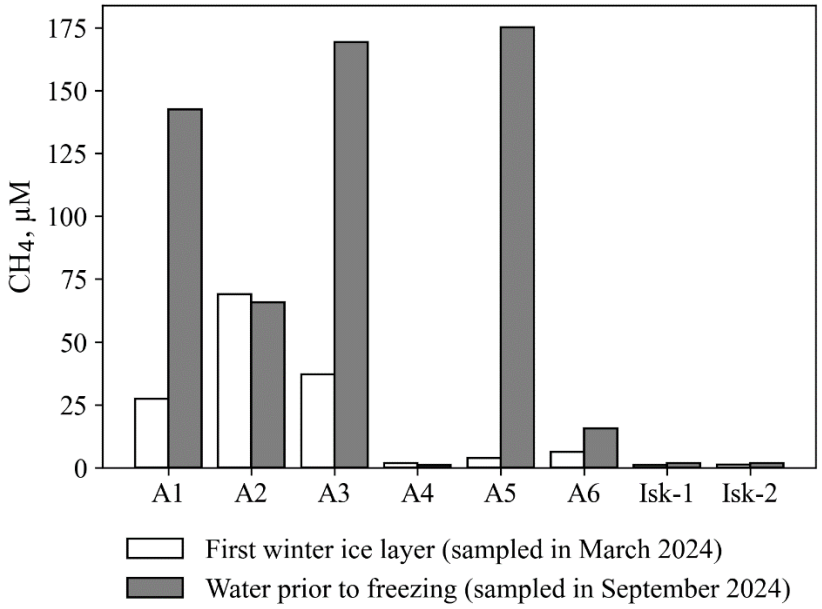

Figure S8. Mean CH_4 concentrations in the first winter ice layer formed (sampled in March 2024) and in the water prior to freezing (sampled in September 2024). Both were calculated using solubility constants corrected for 0°C.

Table S1. Mean pH and Dissolved Organic Content (DOC) of ice layers.

Ice core	Depth from, m	Depth to, m	Description of ice bubbles	DOC, mg L^{-1}	pH
A1	0	0.06	Superimposed	22	5.2
	0.06	0.35	Clear ice	3.6	6.2
	0.35	0.49	Mixed bubbles	3.2	6.2
A2	0	0.13	Ebullition bubbles	3.8	6.6
	0.13	0.22	Spherical and nut shaped bubbles	3.0	6.5
	0.22	0.30	Spherical and nut shaped bubbles	5.4	5.9
	0.30	0.42	Mixed bubbles	3.0	6.1
	0.42	0.46	Mixed bubbles	3.8	5.8
A3	0	0.28	Superimposed	14	6.4
	0.28	0.36	Ebullition bubbles	4.0	6.2
	0.36	0.46	Clear ice	4.8	6.2
	0.46	0.53	Spherical and nut shaped bubbles	4.4	6.3

A4	0	0.25	Ebullition bubbles	3.3	6.0
	0.25	0.33	Mixed bubbles	3.2	6.0
	0.33	0.58	Mixed bubbles	4.4	5.9
A5	0	0.06	Superimposed	17	5.8
	0.06	0.15	Clear ice	3.1	6.1
	0.15	0.22	Spherical and nut shaped bubbles	36	4.9
	0.22	0.39	Mixed bubbles	8.7	5.2
	0.39	0.56	Frozen peat	110	4.4
A6	0	0.27	Superimposed	20	5.6
	0.27	0.40	Clear ice	4.1	5.9
	0.40	0.49	Mixed bubbles	160	4.6
	0.49	0.53	Frozen peat	150	4.4
A7	0	0.13	Clear ice	3.2	6.2
	0.13	0.28	Elongated bubbles	3.4	6.3
	0.28	0.42	Elongated bubbles	2.8	6.1
	0.42	0.58	Mixed bubbles	19	5.4
A8	0	0.06	Superimposed	7.4	8.1
	0.06	0.18	Clear ice	2.1	6.4
	0.18	0.29	Elongated bubbles	2.2	6.2
	0.29	0.45	Elongated bubbles	2.8	6.3
Isk-1	0	0.05	Superimposed	12	4.8
	0.05	0.15	Clear ice	4.6	5.6
	0.15	0.25	Mixed bubbles	3.5	5.6
	0.25	0.37	Mixed bubbles	67	5.0
	0.37	0.5	Mixed bubbles	115	5.3
Isk-2	0	0.06	Superimposed	18	4.9
	0.06	0.22	Clear ice	2.5	5.8
	0.22	0.26	Spherical and nut shaped bubbles	2.7	5.8
	0.26	0.42	Mixed bubbles	6.4	5.6
	0.42	0.55	Mixed bubbles	7.7	5.4

Table S2. Methane (CH_4) storages before ice formation, in the ice column and in water column below ice.

	CH_4 storages, mg CH_4-C m^{-2}			Winter methane bottom flux, mg CH_4-C m^{-2} d^{-1}
	Water column before ice formation	Ice column	Water column below ice	
A1	1326 ± 905	411 ± 62	10303 ± 1372	59 ± 11
A2	1174 ± 86	1580 ± 259	16626 ± 1874	107 ± 14
A3	1364 ± 881	296 ± 76	5524 ± 1008	28 ± 8.6
A4	14 ± 4	1120 ± 147	3347 ± 1349	28 ± 8.7
A5	419 ± 415	5010 ± 473	-	29 ± 4.3
A6	46 ± 23	443 ± 221	-	2.8 ± 1.4
A7	2 ± 1	854 ± 102	-	5.3 ± 0.7
A8	69 ± 67	285 ± 54	5474 ± 1588	36 ± 10
Isk-1	10 ± 4	524 ± 104	(1271 ± 1273) *	3.2 ± 0.7(11 ± 8) *
Isk-2	11 ± 4	1785 ± 319	(636 ± 636) *	11 ± 2.1(15 ± 4.5) *

*The values estimated based on the assumption of dissolved methane storage under the ice in Iškoras pond (Sect. 3.5).

Table S3. Mean CH_4 ice-free flux measured for ponds by the eddy covariance tower at the Iškoras site (Pirk et al., 2024) over three years (2019-2021). The ice-free period was defined as June 10 to September 10 to exclude contributions from ice melt and autumn turnover. The mean temperature of the pond during this period in 2023 was 11.4°C.

Year	Ice-free CH_4 flux, mg CH_4-C m^{-2} d^{-1}			
	mean	std	25th	75th
2019	37	20	24	49
2020	40	22	25	54
2021	39	20	26	53

References

Norgeibilder.no: Statens kartverk, Geovekst og kommunene: Kautokeino 1958, Alta Kautokeino riksgrensen 1966, Roavvoaivi 2003, Finnmark 2013, Karasjok 2003, Finnmark 2011, https://www.norgeibilder.no/, last access: 03 June 2025.

Pirk, N., Aalstad, K., Mannerfelt, E. S., Clayer, F., De Wit, H., Christiansen, C. T., Althuizen, I., Lee, H., and Westermann, S.: Disaggregating the Carbon Exchange of Degrading Permafrost Peatlands Using Bayesian Deep Learning, Geophysical Research Letters, 51, e2024GL109283, https://doi.org/10.1029/2024GL109283, 2024.